Sticking Coefficient and Processing of Water Vapor on Organic-Coated Nanoaerosols

Purnendu Chakraborty and Michael R. Zachariah*

Department of Mechanical Engineering and Department of Chemistry and Biochemistry, University of Maryland, College Park, Maryland, and National Institute of Standards and Technology, Gaithersburg, Maryland

Received: August 10, 2007; In Final Form: October 11, 2007

Organic-based aerosols may play an unexpectedly important role in the atmospheric processing of water vapor. In this paper, we report results of a molecular dynamics (MD) study on the sticking coefficient of water vapor on a coated particle (water droplet coated with fatty acid of radius ∼4 nm). The sticking coefficient was found to be almost a constant (11−16%) for incident speeds around the most probable speed as opposed to 100% for water vapor incident on a pure water droplet. The sticking coefficient was found to increase with the size of the water cluster (water-*N*mer) impinging the surface of the particle and was seen to approach 1 for impinging water clusters consisting of 10 molecules or more. We also computed the average energy transferred per collision for monomers impinging the surface of the coated particle and found the value to be 4.4581 kJ/mol. Most important perhaps was the fact that despite the lower sticking coefficient, the equilibrium vapor pressure of water over these inverted micelles was considerably lower due to the surface tension effects of the fatty acid layer. As such, these coated particles act as effective substrates for water vapor condensation and may play a role as cloud condensation nuclei.

Introduction

Aerosol particles are ubiquitous in the earth's atmosphere and have a major influence on global climate and perhaps climate change. They can locally either intensify or moderate the effects of the greenhouse gases through scattering or absorption of both incoming solar radiation and thermal radiation emitted from earth's surface. Aerosols also act as cloud condensation nuclei and thereby affect the radiative properties of clouds.[1] Marine aerosol particles play an important role in atmospheric processes. It has recently been shown[2,3] using time-of-flight secondary mass spectrometry (TOF−SIMS) that fatty acids reside on surfaces of sea-salt aerosols. In a subsequent work[4] the ubiquity of fatty acid population on a variety of continental aerosols was reported.

A conceptual model has been suggested[5] for the composition, structure, and atmospheric processing of organic aerosols. In the proposed model organic aerosol is an "inverted micelle" consisting of an aqueous core that is encapsulated in an inert, hydrophobic organic monolayer. The organic materials that coat the aerosol particles are surfactants of biological origin. In this model the surfactants lie with their polar heads inserted into the ionic aqueous core, with their hydrophobic hydrocarbon tails exposed to the atmosphere. More recently Wyslouzil et al.[6] has shown, using small-angle neutron scattering, evidence for surface segregation of organic/water systems, and Li and Wilemski[7] using Monte Carlo methods mapped out the stability regions of binary water/organic droplets. Understanding the structure and properties of these coated aerosols is important as they may affect the processing of water vapor in the atmosphere, cloud formation, and the radiation balance to the earth.

In a recent work,[8] using coarse-grained[9−11] molecular dynamics (MD) simulation, we observed that these particles indeed favor an inverted micelle like structure. This structure results in a radial pressure profile (see Figure 1 which is a reproduction of Figure 3 of our prior work[8]) such that the coating is under negative pressure, i.e., tension. Using a simple geometric model and force balance, we showed that this negative pressure is a manifestation of the curved surface. *This negative normal pressure corresponded to a "negative" surface tension.* Now, the equilibrium vapor pressure over a small particle is higher than that over a flat surface and is given by the Kelvin equation $\ln p/p_S = 2\gamma\bar{v}/r_pRT$, where p is the actual pressure of the vapor, p_S is the equilibrium vapor pressure for a planar surface, r_p is the droplet radius, γ is the surface tension, $\bar{v}$ is the molar volume of the liquid, R is the gas constant, and T is the temperature. Normally, for a small particle, $p > p_S$. However, if γ were indeed negative, we will get $p < p_S$, i.e., the vapor pressure of the particle is reduced due to the coating, and such a coated particle would act as an enhanced condensation surface. Indeed, we observed that water vapor introduced in the simulation cavity containing the coated particle was absorbed. Thus, despite the hydrophobic coating, such organic-coated aerosols can possibly act as a very efficient substrate to process water vapor. The implication of course is that such a structure may be important as a cloud condensation nucleus.

In this paper we make a systematic study of the water processing by the coated particles, compute the rate of water uptake, and show that these structures indeed will enhance water nucleation.

Computational Model and Simulation Details

All the MD simulations in this work were performed using the GROMACS[12−14] simulation software package implemented on a parallel architecture. For this work, we used the SPC/E water model[15,16] that consists of a tetrahedral water model with an OH distance of 0.1 nm, with point charges on the oxygen and hydrogen positions of equal to −0.8476 and +0.4328 e

* Corresponding author. E-mail: mrz@umd.edu.

10.1021/jp076442f CCC: $40.75 © 2008 American Chemical Society
Published on Web 01/15/2008

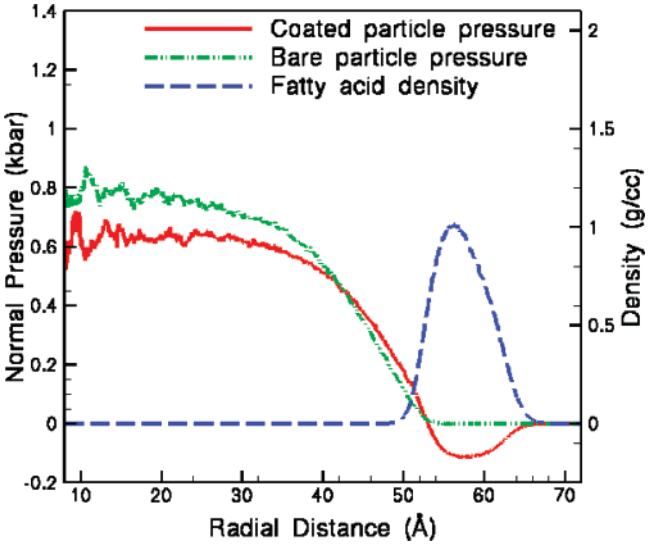

Figure 1. Pressure profiles of bare and coated particles. The dashed (blue) curve represents the fatty acid density. It is evident from the plot that while the interior of the particle is under compression, the coating is under negative pressure, i.e., tension. Reprinted from ref 8. Copyright 2007 American Chemical Society.

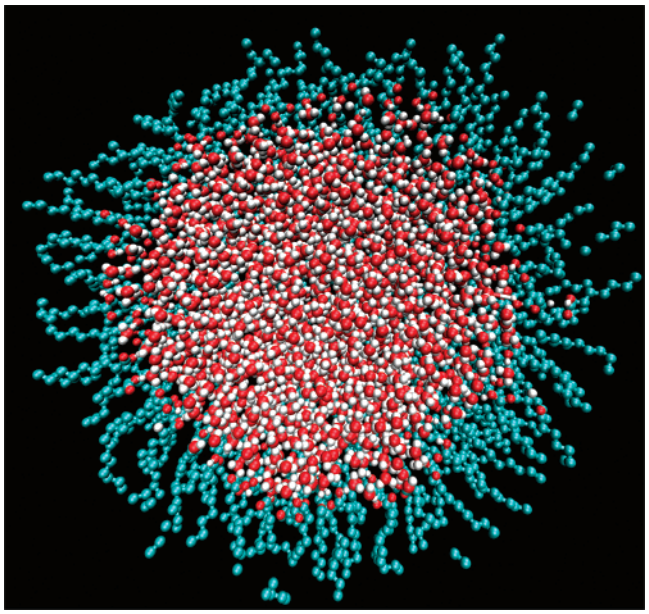

Figure 2. Cross-sectional view of an equilibrated coated particle at 260 K (consisting of 2440 water molecules and 505 fatty acid molecules).

(electronic charge units), respectively, and a Lennard-Jones interaction on the oxygen positions, given by

$$V_{LJ}(r_{ij}) = -\left(\frac{A}{r_{ij}}\right)^6 + \left(\frac{B}{r_{ij}}\right)^{12} \quad (1)$$

with $A = 0.37122$ (kJ/mol)$^{1/6}$ nm, $B = 0.3428$ (kJ/mol)$^{1/12}$ nm, and r_{ij} being the distance between two oxygen atoms. An analytical version of the SHAKE algorithm[17] was used to maintain the rigidity of the water molecules. Dodecanoic (lauric) acid [CH_3–$(CH_2)_{10}$–COOH] was chosen as our model fatty acid system. The fatty acid molecules were modeled using both the "united atom" setup (each CH_2 group was represented by a single site with interactions defined between these sites) and the "fully atomistic" setup (to represent the −COOH group). For force calculations the switched Lennard-Jones (the potential

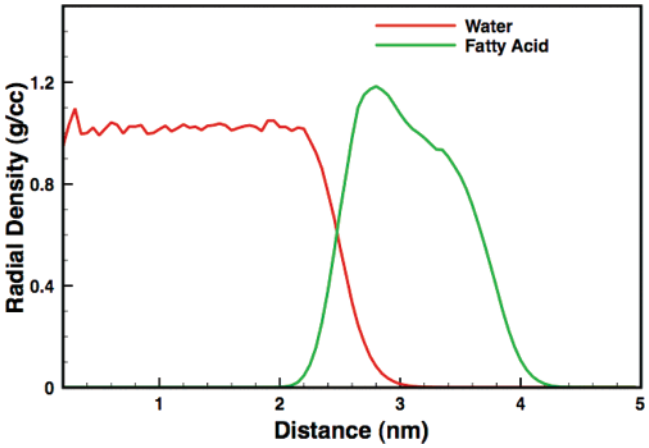

Figure 3. Radial density profiles of the coated particle. Distance is measured radially outward from the center of mass of the particle.

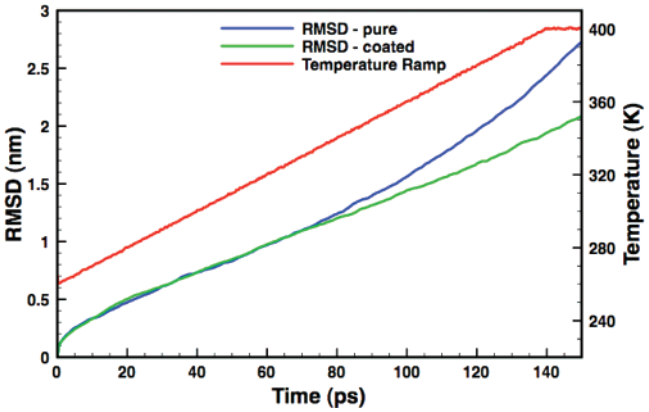

Figure 4. Root-mean-square deviations of water molecules in the pure and coated particles during a heating ramp (red line).

is normal up to 0.9 nm, after which it is switched off to reach zero at a distance of 1 nm) was used to model the van der Waals interactions The (switched) Coulombic potential was used for interaction between charges. The equations of motion were integrated using leap-frog algorithm with a time step of 1 fs. The simulations were typically conducted on 2−4 processors running in parallel, with a neighbor list cutoff distance of 1.3 nm. Unless otherwise mentioned, all the simulations were conducted in vacuum (with no periodic boundary conditions). For temperature control, the system was coupled to an external bath at the desired temperature using "berendsen" coupling with a coupling constant of 1 fs (equal to the time step).

Structure

The first step toward building an equilibrated coated particle was to build a pure water droplet. We first generated a simple cubic structure (with the oxygen atom at the vertex of each cube) and then considered only the water molecules inside a sphere of a certain radius, thereby generating a spherical initial configuration consisting of 2440 water molecules. Generating velocities corresponding to 200 K, an equilibration simulation was run for 50 ps. The particle was then slowly heated to 260 K over a period of 120 ps. Finally, a constant temperature simulation is run for 100 ps keeping the temperature constant at 260 K. The radial distribution function, confirms the liquid state (the peak occurs at the expected distance of 2.8 Å). Fatty acid molecules were then attached to the surface water molecules to coat the water droplet. The polar part of the fatty acid molecule was attached to a surface water molecule with the

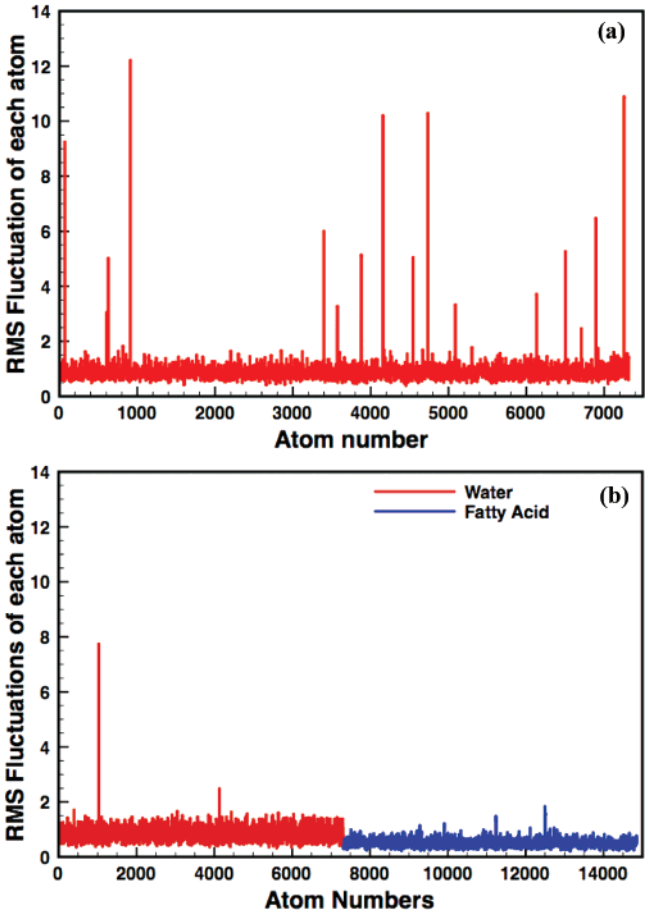

Figure 5. (a) Root-mean-square fluctuations of each atom in the pure water droplet resulting from heating. (b) Root-mean-square fluctuations of each atom in the coated droplet resulting from heating.

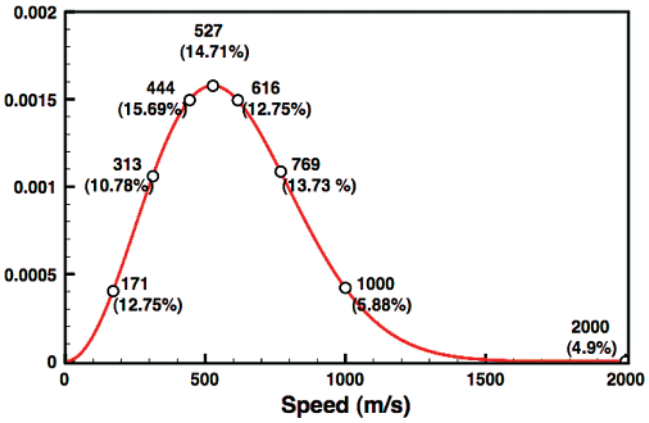

Figure 6. Sticking coefficients of the water monomer for various values of incident speeds on a Maxwell−Boltzmann speed distribution at 300 K. Percent values in parentheses are the fraction of sticking collisions at the given speed.

hydrocarbon tail placed radially outward. Velocities were initialized for these fatty acid molecules corresponding to a temperature of 260 K, and the coated particle was allowed to equilibrate. Due to difficulties with identifying the surface water molecules, some of these fatty acid molecules overlap and experience a strong repulsive force and, hence, were released from the particle. Fatty acid molecules that left the droplet were removed from the simulation, and a constant temperature (260 K) simulation was run for 100 ps. Figure 2 shows a cross-sectional view of the equilibrated coated particle consisting of

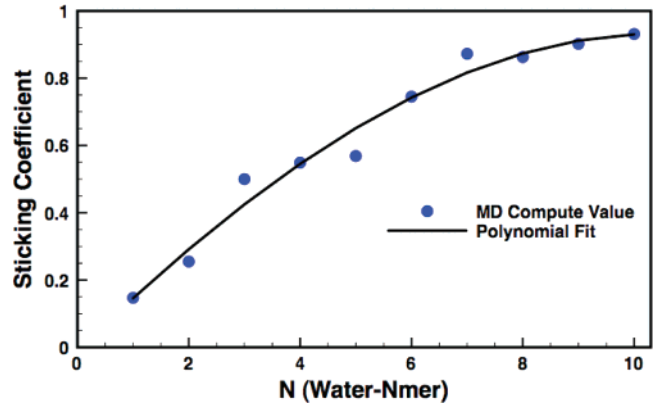

Figure 7. Sticking coefficients for water-*N*mers of different sizes for different values of *N*.

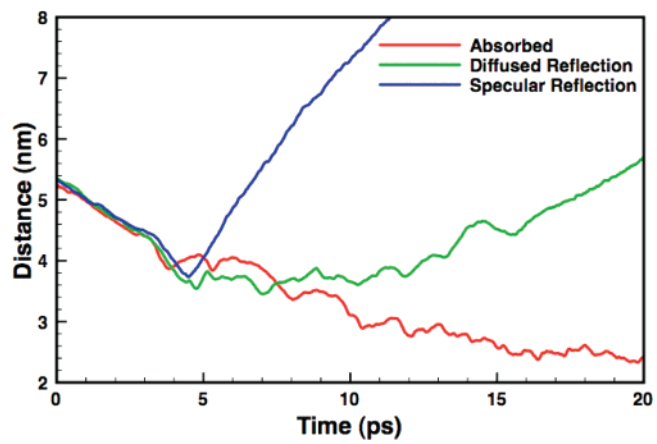

Figure 8. Distance of the center of mass of the incident monomer from the center of mass of the coated particle plotted as a function of time for the three types of interactions.

2440 water molecules and 505 fatty acid molecules. The coated particle was next heated to 300 K and equilibrated at that temperature.

Results and Discussion

Density. The radial density profile was computed[18] as a function of *r*, the distance from the center of mass of the particle. To compute density, we introduced subspherical shells (centered at the center of mass of the coated particle) at a distance of $\delta r = 0.05$ nm from each other. The density at a distance *r* from the center of mass was computed as the mass of all the atoms in the shell between radii *r* and $r + \delta r$ divided by the volume of the shell. Figure 3 shows the density plot for the coated droplet. As we had seen in our earlier[8] work, the particle exhibits a core−shell like structure with an aqueous core encapsulated in an inert hydrophobic organic monolayer. The fatty acid molecules stay on the surface of the water droplet forming a hydrophobic coating. As we had pointed out this structure is mechanically stable.

Effect of Heating on Stability. We tested the stability of both the bare and the coated particles by heating them slowly from 260 to 400 K (the temperature ramp for both the pure and the coated particles over time is shown is Figure 4). To quantify stability we computed the rmsd (root-mean-square deviation),

$$\mathrm{rmsd}(t) = \left[\frac{1}{N^2}\sum_{i=1}^{N}\sum_{j=1}^{N}|\mathbf{r}_{ij}(t) - \mathbf{r}_{ij}(0)|^2\right]^{1/2} \qquad (2)$$

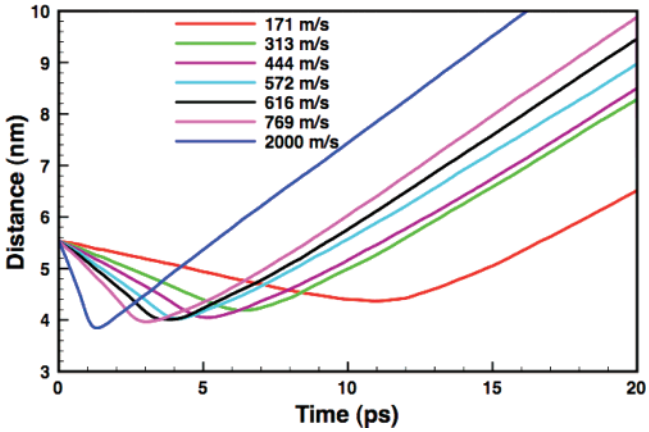

Figure 9. Plot of the distance of the center of mass of the monomer from the center of mass of the coated particle vs time. Each trajectory obtained has been averaged over all the reflected trajectories for a given incident speed.

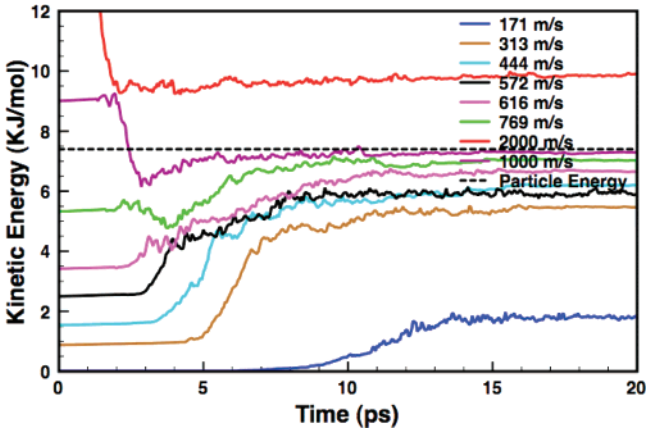

Figure 10. Plot of the change in kinetic energy (KE) of a monomer vs time. Each trajectory has been averaged over all the reflected trajectories for a given incident speed. The "dashed" line represents the thermal energy of the coated particle.

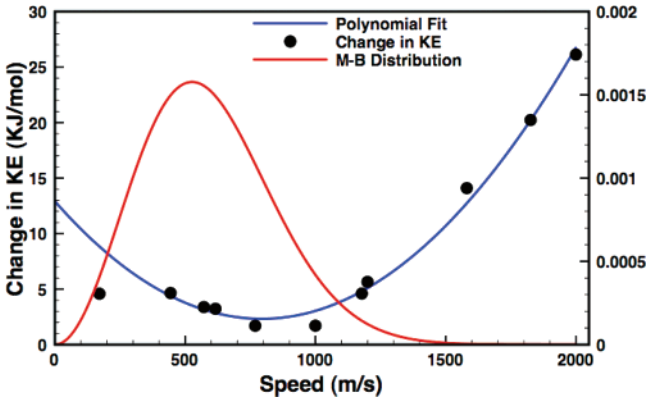

Figure 11. Change in KE is plotted for each incident speed case. The blue line is a polynomial (degree 2) fit to the change in KE data and is used to compute the average energy transferred per collision. Also plotted is the Maxwell−Boltzmann distribution for a water monomer at 300 K.

where the distance $\mathbf{r}_{ij}$ between N atoms at time t is compared with the distance between the same atoms at time 0. The rmsd of water molecules as a function of time for both the pure and the coated particles was computed and is plotted in Figure 3. Evidently, and as expected, the fatty acid coating increased the stability of the water droplet. Although the rmsd for both materials increased with temperature there is a clear bifurcation at about 300 K where the water droplet rmsd exceeds that of the coated drop. The rmsf (root-mean-square fluctuations), defined as the standard deviation (from the original equilibrated structure) of atomic positions of each of the atoms in the particles, were also computed for both the particles. Figure 5, panels a and b, plots the rmsf for both types of particles. The x-axis of the plots lists the atom indexes (2440 water molecules implying 7320 atoms) and the y-axis is the measure of the fluctuation in nm. The median of the deviations is 0.84 nm. In the case of the pure water droplet 16 water molecules were seen to evaporate as a result of the heating, as compared with just 2 water molecules evaporating in the case of the coated particle for the same temperature ramp confirming the fact that the water molecules in the coated droplet are far more stable than their counterparts in the pure droplet. Heating the pure water droplet to 300 K results in some evaporation from the surface. However, the coated particle is stable at 300 K (no evaporation takes place over a period of 100 ps), and we have used the coated particle at this temperature for the subsequent computation of the sticking coefficient and average energy transferred per collision. The sticking coefficient calculations were carried out at a constant temperature of 300 K, whereas the energy transfer calculations were done in a constant energy environment.

Water Vapor Sticking Coefficient. The sticking (mass accommodation) coefficient or sticking probability, α, describes the probability of the gas molecule being incorporated into the liquid[19]

$$\alpha = \frac{\text{number of molecules absorbed into liquid}}{\text{number of molecules impinging the liquid surface}} \quad (3)$$

An accurate determination of the sticking probability is important since it is directly relevant to the nucleation and growth kinetics of cloud droplets, and subsequently climate change.[20,21] Vieceli et al.[19] computed the sticking coefficient of a gas-phase water molecule, approaching the surface of liquid water (flat surface) with a thermal impact velocity, and obtained a value of effectively unity (0.99 at 300 K). Morita et al.[22] computed the mass accommodation coefficient of water vapor into liquid water (flat surface) and found the value of α to be >0.99 at 273 K. The sticking probability of water vapor onto an organic-coated spherical water droplet has not been computed to the best of our knowledge.

To address this point we carried out a water processing simulation in which we placed water vapor outside the particle with a random velocity (sampled from the Maxwell−Boltzmann distribution) corresponding to the desired temperature.

A water monomer (single water molecule) was placed at a distance of 6 nm from the center of the coated particle, outside the potential cutoff distance so that initially there is no force acting between the monomer and the coated particle. The molecule was then given a velocity vector toward the center of mass of the coated particle. For each incident speed, sampled at random from the Maxwell−Boltzmann speed distribution at 300 K, Figure 6, 102 separate trajectories were considered by placing the water monomer along the sphere of radius 6 nm. The sticking coefficient was computed as the ratio of the number of monomers trapped on the coated particle to the number of monomers impinging on the surface (102 in the present case). The trajectory of each monomer was monitored for 60 ps, and this process was repeated for all collision events. The incident water molecule was considered trapped on the particle if the distance of the center of mass of the monomer from the center of mass of the particle was less than 5 nm; else it was considered an unreactive event.

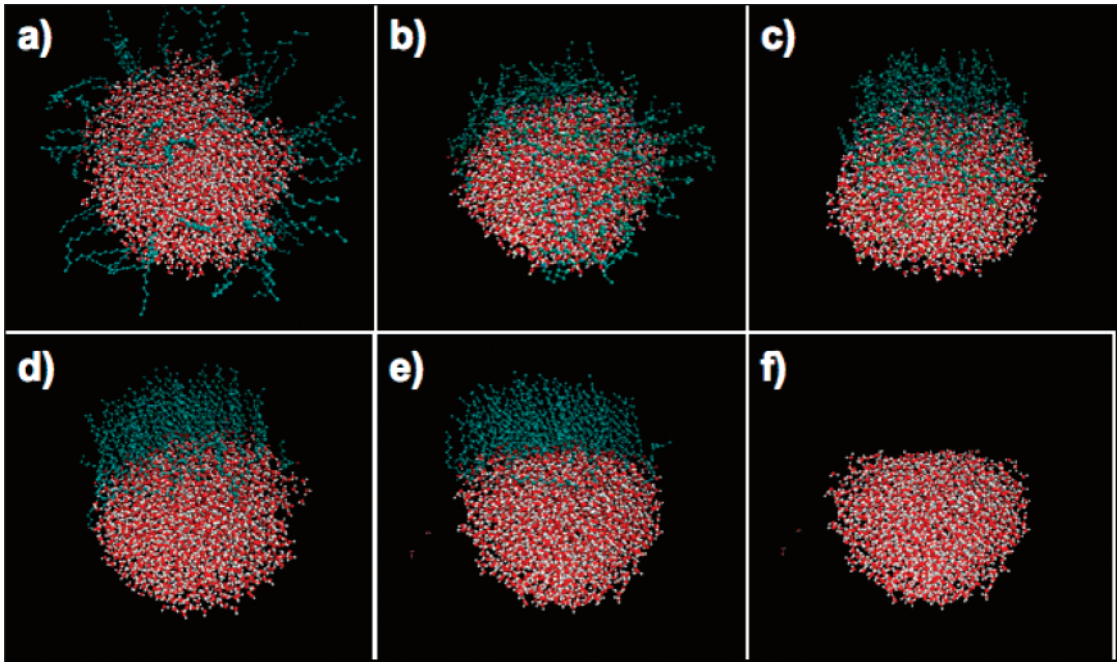

Figure 12. (a−e) Snapshots of the equilibration process of a particle consisting of 2440 water and 101 fatty acid molecules. (f) The snapshot of the final equilibrated structure without the fatty acid molecules (emphasizing the flat interface).

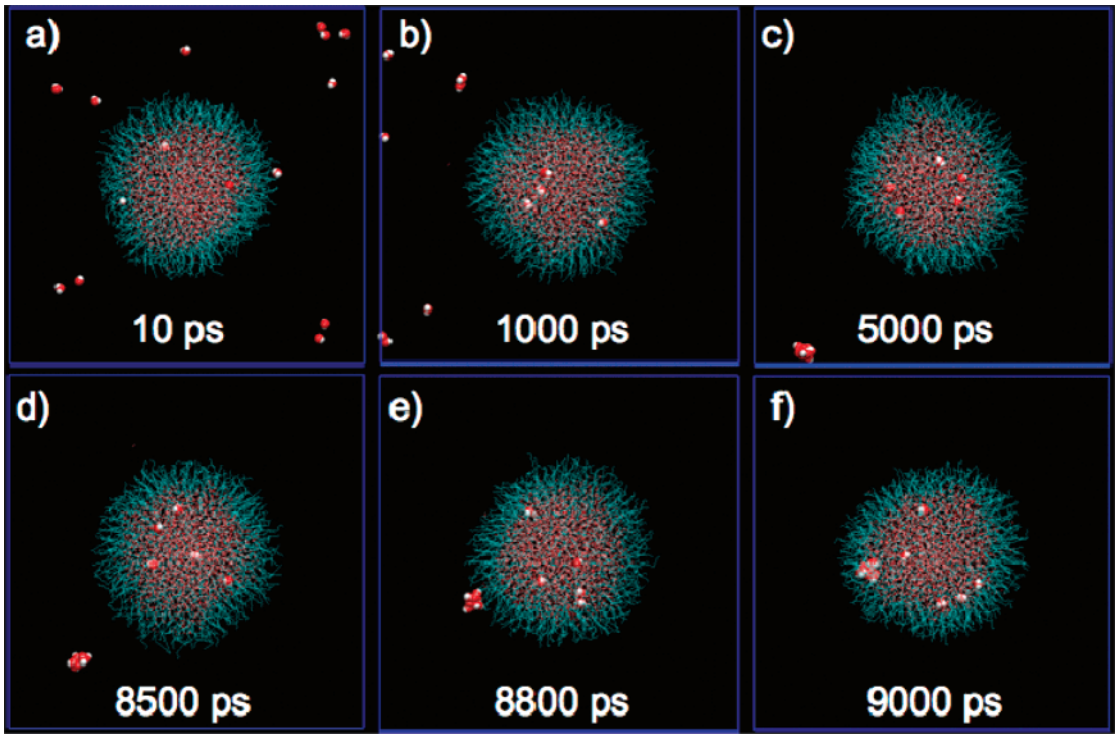

Figure 13. (Orthographic) snapshots of various stages of the 20 ns simulation to test the reduction in vapor pressure because of the coating. Larger spheres are used to represent the water molecules in the vapor phase.

Figure 6 shows the percentage of monomers (i.e., sticking coefficient, presented as percentages within parentheses) that get trapped on the particle for each of the incident energies considered. The sticking coefficient is essentially a constant (within 5%) for incident speeds around the most probable speed and reduces significantly at higher incident speeds (>1000 m/s). In general, the results indicate that approximately 1 in every 6−7 encounters results in water condensation. Next, we carried out the same trajectory calculations with the equilibrated pure water particle and placing the incident water monomer at a distance of 5 nm from the center of the particle (this time the trajectories were calculated at a temperature 260 K with speeds sampled from the corresponding Boltzmann distribution). For the pure water droplet, all the incident monomers were absorbed into the water droplet implying that the pure water droplet has a sticking coefficient of 1.

Finally, we considered a sequence of water-*N*mers of different sizes ($N = 1$ for monomers, $N = 2$ for dimers, etc.) each shot toward the center of the particle with its corresponding most probable speed (as determined from the Maxwell−Boltzmann distribution). Figure 7 plots the sticking coefficients (at the most probable speed) as a function of the water-*N*mer size (*N*). We

find that the sticking coefficient increases smoothly with increasing water-mer size and approaches 1 for $N > 10$.

Energy Transferred Due to Collision of a Monomer with the Coated Particle. For a monomer colliding with the coated particle, we noticed three types of collisions.[23] The incident water monomer either underwent (i) immediate (almost specular) reflection upon contact, or (ii) it underwent surface diffusion and eventually gained enough energy to desorb from the surface (diffused reflection), or (iii) it penetrated through the fatty acid coating and was absorbed into the water core of the particle. These three cases are illustrated in Figure 8, which plots the time evolution of the distance of the center of mass of the monomer from the center of mass of the particle (the curves shown are typical examples of each case). Subsequently, for each incident speed case, the average distance of the monomer from the particle was computed (the average being taken over all the reflected trajectories, including both the specular and diffuse reflection cases). The result is summarized in Figure 9. It is evident that the monomers with higher incident energies spend less time on the surface of the particle and undergo a more specular reflection and less energy accommodation. It is interesting to note that the higher energy monomers penetrate the surface of the coated particle more than their lower energy counterparts. On an average the monomers with incident speed of 2000 m/s travel a distance of 0.5 nm deeper into the coating than those with an incident speed of 171 m/s.

Next, for each incident speed case, we computed the change in the total kinetic energy (KE) due to collision. Toward that end we tracked the KE for all the trajectories and took an average of the KE over all the reflected trajectories. Figure 10 plots the (averaged) time evolution of KE for each incident speed case. As expected, monomers with incident energy lower than the thermal energy of the particle gain energy from the particle resulting in a positive change in KE, whereas for the monomers impinging the particle with a higher energy, the change in energy is negative. The absolute value of this change in KE (ΔE = final KE − initial KE) is plotted in Figure 11 (black circles). To obtain a functional form for $|\Delta E|$, we fitted a polynomial of degree 2 to this MD computed data (represented by the blue line in Figure 11). Using this fitted functional form of $|\Delta E|$, we computed the average energy transferred per collision as

$$\langle \Delta E^2 \rangle^{1/2} = \left(\int_0^\infty (\Delta E^2) f(v)\, \mathrm{d}v\right)^{1/2} \tag{4}$$

where $f(v)$ is the Maxwell−Boltzmann distribution of speed (Figure 11). The computed value of the average energy transferred per collision is 4.4581 kJ/mol, i.e., 372.67 cm^{-1}. This value is consistent with the value obtained[24] for a highly excited polyatomic colliding with a monatomic bath gas.

Negative Surface Tension and Reduction in Vapor Pressure. As mentioned earlier, coated particles with core−shell structure would act as if the surface tension is negative[8] and is a direct consequence of the fatty acid molecules being under tension, which gives rise to a negative normal pressure profile in that region. Mechanically this effect occurs because the effective density of fatty acid chains decrease as one moves radially out from the anchor point of the chains at the water interface. This latter point was demonstrated using a simple geometrical argument and force balance.[8] A negative surface tension implies that a particle would tend to increase its surface area, possibly by deformation, so that a majority of the fatty acid molecules line up parallel to each other (thereby reducing the tension in the coating). This phenomenon is, however, never seen with fully coated particles because of the high concentration of fatty acid molecules on the surface of the particle resulting in a large interfacial tension, which maintains the spherical shape of the particle. As an example we removed 80% of the fatty acid molecules from the surface of the fully coated particle (the resulting particle consisted of 2440 water molecules and 101 fatty acid molecules) and let the system equilibrate for 20 ns. Figure 12a−e shows snapshots of this simulation. Figure 12a shows the initial particle. The fatty acid molecules that were initially spread out on the surface of the particle diffuse and nucleate to form a monolayer on a part of the droplet. Figure 12e shows the equilibrated structure where the fatty acid molecules line up parallel to each other on a locally flat surface (Figure 12f). From Figure 12f it is evident that although the rest of the water surface maintains a roughly spherical shape, the part of the surface in contact with fatty acid becomes flat enabling the fatty acid molecules to line up.

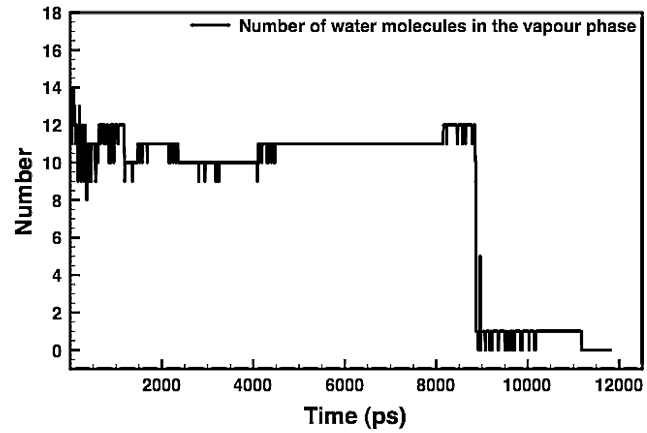

Figure 14. Plot of the number of water molecules in the vapor phase as a function of time.

One direct implication of the "negative" surface tension is that it reduces the equilibrium water vapor pressure. As a result a coated particle would act as an effective substrate for water condensation despite its hydrophobic surface. To test this, a pure water droplet, equilibrated at 260 K, was placed in the center of a cubic box of edge 15 nm with periodic boundary conditions, heated slowly to 300 K (over a period of 120 ps), and maintained for another 5 ns. The water droplet reaches equilibrium by evaporating some of the water so that at steady state on an average 14 water molecules exist in the vapor phase. A water molecule was considered to be in the vapor phase if its distance from the center of particle exceeded 6 nm. This corresponds to an equilibrium vapor pressure of 0.15 atm. Next, the water droplet was replaced with the coated droplet (at 300 K), and 14 water molecules, in the vapor phase, were added to the system. The system was then allowed to evolve for a total of 20 ns. Figure 13 shows snapshots of this simulation. In the figure, the water molecules in the vapor phase have been represented by larger spheres for easy identification. Figure 13a is a snapshot taken soon after the start of the simulation. In the first 20 ps two vapor molecules penetrate the coating of the particle and get absorbed into the water core of the particle. The rest of the vapor molecules were seen to be reflected off the surface of the particle. Over a period of the next 8 ns, the 12 vapor molecules came together to form a water-12mer. This water cluster, upon striking the surface of the particle (Figure 13, panels d and e), was completely absorbed (Figure 13f) into the water core of the particle (sticking coefficient is ∼1 for water-*N*mers with $N > 10$, Figure 6). Figure 14 plots the number of water molecules in the vapor phase as a function of time. The implications of this computer experiment are clear. (1) The

equilibrium vapor pressure of water is considerably lower in the presence of the coated particles. Indeed it was sufficiently low that it induced homogeneous nucleation to occur in the simulation box. (2). Determining the actual equilibrium vapor pressure is not feasible using a traditional MD approach at ambient temperatures, because it would require an exceedingly large simulation box to obtain the low water vapor density so that the evaporation and condensation rates match. Indeed over the simulation times investigated in this paper we never observed a water molecule to evaporate from a coated particle at 300 K. This latter point is interesting in that the vapor pressure of these inverted micelles structures is very low despite the fact that the sticking coefficient is about one-sixth that of a pure water−water drop encounter.

Conclusion

This study was motivated by a prior simulation in which water−fatty acid mixtures lead to inverted micelle structures.[8] These structures in turn show unusual surface properties, namely, an "effective" negative surface tension, which implies that they would attract water. Molecular dynamics simulation was used to determine the sticking coefficient of water vapor on a water droplet coated with fatty acid at 300 K. The sticking coefficient was found to be almost a constant (11−16%) for incident speeds around the most probable speed as opposed to 100% for water vapor incident on a pure water droplet. The sticking coefficient was found to increase with the size of the water cluster (water-*N*mer) impinging the surface of the particle and was seen to approach 1 for impinging water clusters consisting of 10 molecules or more.

The most important result was that despite the lower sticking coefficient these materials result in a much lower equilibrium water vapor pressure, and as such these coated particles act as effective substrates for water vapor condensation and may play a significant role as cloud condensation nuclei.

References and Notes

(1) Buseck, P. R.; Posfai, M. Airborne minerals and related aerosol particles: Effects on climate and the environment. *Proc. Natl. Acad. Sci. U.S.A.* **1999**, *96*, 3372.

(2) Tervahattu, H.; Hartonen, K.; Kerminen, V.-M.; Kupiainen, K.; Aarnio, P.; Koskentalo, T.; Tuck, A. F.; Vaida, V. New evidence of an organic layer on marine aerosols. *J. Geophys. Res. (Atmos.)* **2002**, *107* (D7), 4053.

(3) Tervahattu, H.; Juhanoja, J.; Kupiainen, K. Identification of an organic coating on marine aerosol particles by TOF-SIMS. *J. Geophys. Res. (Atmos.)* **2002**, *107* (D16), 4319.

(4) Tervahattu, H.; Juhanoja, J.; Vaida, V.; Tuck, A. F.; Niemi, J. V.; Kupianien, K.; Kulmala, M.; Vehkamaki. Fatty acids on continental sulfate aerosol particles. *J. Geophys. Res.* **2005**, *110* (D06207).

(5) Ellison, G. B.; Tuck, A. F.; Vaida, V. Atmospheric processing of organic aerosols. *J. Geophys. Res.* **1999**, *104* (D9), 11633.

(6) Wyslouzil, B. E.; Wilemski, G.; Strey, R.; Heath, C. H.; Dieregsweiler, U. Experimental evidence for internal structure in aqueous−organic nanodroplets. *Phys. Chem. Chem. Phys.* **2006**, *8*, 54−57.

(7) Li, S.; Wilemski, G. A structural phase diagram for model aqueous organic droplets. *Phys. Chem. Chem. Phys.* **2006**, *8*, 1266.

(8) Chakraborty, P.; Zachariah, M. R. "Effective" negative surface tension: A property of coated nanoaerosols relevant to the atmosphere. *J. Phys. Chem. A* **2007**, *111*, 5459−5464.

(9) Shelley, J. C.; Shelley, M. Y.; Reeder, R. C.; Bandyopadhyay, S.; Klein, M. L. A coarse grained model for phospholipid simulations. *J. Phys. Chem. B* **2001**, *105*, 4464−4470.

(10) Shelley, J. C.; Shelley, M. Y.; Reeder, R. C.; Bandyopadhyay, S.; Moore, P. B.; Klein, M. L. Simulations of phospholipids using a coarse grain model. *J. Phys. Chem. B* **2001**, *105*, 9785−9792.

(11) Lopez, C. F.; Moore, P. B.; Shelley, J. C.; Shelley, M. Y.; Klein, M. L. Computer simulation studies of biomembranes using a coarse grain model. *Comput. Phys. Commun.* **2002**, *147*, 1−6.

(12) van der Spoel, D.; Lindahl, E.; Hess, B.; van Buuren, A.; Apol, E.; Tieleman, P.; Meulenhoff, P.; Sijbers, A.; Feenstra, A.; Drunen, R.; Berendsen, H. *Gromacs User Manual*, version 3.2. www.gromacs.org, 2004.

(13) Berendsen, H. J. C.; van der Spoel, D.; van Drunen, R. GROMACS: A message-passing parallel molecular dynamics implementation. *Comput. Phys. Commun.* **1995**, *91*, 43−56.

(14) Lindahl, E.; Hess, B.; van der Spoel, D. Gromacs 3.0: A package for molecular simulation and trajectory analysis. *J. Mol. Model.* **2001**, *7*, 306−317.

(15) Berendsen, H. J. C.; Postma, J. P. M.; van Gunsteren, W. F.; Hermans, J. Interaction Models for Water in Relation to Protein Hydration. In *Intermolecular Forces*; Pullman, B., Ed.; Reidel: Dordrecht, The Netherlands, 1981; p 331.

(16) Berendsen, H. J. C.; Grigera, J. R.; Straatsma, T. P. The missing term in effective pair potentials. *J. Phys. Chem.* **1987**, *91*, 6269.

(17) Miyamoto, S.; Kollman, P. A. Settle: An analytical version of the Shake and Rattle algorithms for rigid water models. *J. Comput. Chem.* **1992**, *13*, 952.

(18) Thompson, S. M.; Gubbins, K. E.; Walton, J. P. R. B.; Chantry, R. A. R.; Rowlinson, J. S. A. Molecular Dynamics study of liquid drops. *J. Chem. Phys.* **1984**, *81*, 530.

(19) Vieceli, J.; Roeselova, M.; Tobias. D. J. Accommodation coefficients for water vapor at the air/water interface. *Chem. Phys. Lett.* **2004**, *393*, 249−255.

(20) Chuang, P. Y.; Charlson, R. J.; Seinfeld, J. H. Kinetic limitations on droplet formation in clouds. *Nature* **1997**, *390*, 594.

(21) Nenes, A.; Ghan, S.; Abdul-Razzak, H.; Chuang, P. Y.; Seinfeld, J. H. Kinetic limitations on cloud droplet formations and impact on cloud albedo. *Tellus* **2001**, *53B*, 133.

(22) Morita, A.; Sugiyama, M.; Kameda, H.; Koda, S.; Hanson, D. R. Mass accommodation coefficient of water: Molecular dynamics simulation and revised analysis of droplet train/flow reactor experiment. *J. Phys. Chem. B* **2004**, *108* (26), 9111−9120.

(23) Li, Z.; Wang, H. Gas−nanoparticle scattering: A molecular view of momentum accommodation function. *Phys. Rev. Lett.* **2005**, *95*, 014502.

(24) Gilbert, R. G.; Smith, S. C. *Theory of Unimolecular and Recombination Reactions*; Blackwell Scientific Publications: Oxford, London, 1990.